

Magnetotransport as a probe of phase transformations in metallic antiferromagnets: the UIrSi_3 case

F. Honda¹, J. Valenta², J. Prokleška², J. Pospíšil², P. Proschek², J. Prchal², and V. Sechovský²

¹*Tohoku University, Institute for Materials Research, Narita-cho 2145-2, Oarai, Ibaraki, Japan*

²*Charles University, Faculty of Mathematics and Physics, Department of Condensed Matter Physics, Ke Karlovu 5, Prague 2, Czech Republic*

Abstract

The electrical resistance and Hall resistance of the Ising-like non-centrosymmetric antiferromagnet UIrSi_3 were measured as functions of temperature and magnetic field. The unequivocally different character of first-order and second-order magnetic phase transitions in UIrSi_3 has been found leading to distinctly different transport properties in the neighborhood of the corresponding critical temperatures and magnetic fields. Considering the magnetic part of electrical resistivity and Hall resistivity in contributions of three magnetic regimes we suggest a scenario which may successfully explain the observed change of polarity of the phase-transition accompanying contributions at tricritical point in the magnetic phase diagram of UIrSi_3 . The observed anomaly in the field-dependence of electrical resistivity below 4 T at low temperatures indicates existence of an additional field-induced antiferromagnetic phase. It leads to extension of the magnetic phase diagram of UIrSi_3 presented in this paper. The results of our study emphasize the usefulness of measurements of electrical transport as a sensitive probe of magnetic phase transformations in antiferromagnets sometimes hardly detectable by other methods.

Introduction

Since the electrical transport can be influenced by interactions of conduction electrons with magnetic fields and with unpaired electrons carrying magnetic moments electrical and Hall resistivity may serve as important probes of details of magnetism in metallic materials.

The electrical resistivity ρ in magnetic metals is considered within a simple approach, supposing validity of Mathiessens' rule, as a sum:

$$\rho = \rho_0 + \rho_{e-p} + \rho_{mag} \quad (1).$$

The temperature independent residual-resistivity term ρ_0 which originates in the scattering of conduction electrons on lattice defects and the electron-phonon term ρ_{e-p} reflecting the scattering of conduction electrons on phonons are present in all metallic materials. The latter term represents the scattering of conduction electrons on magnetic moments due exchange interaction with unpaired electrons carrying the moment. In systems with localized magnetic moments, e.g. lanthanide 4f-electron moments, ρ_{mag} is expected by theory to scale with the de Gennes factor $(g-1)^2 J(J+1)$ and with the square of the exchange coupling parameter \mathcal{J} ¹. In a paramagnetic (PM) range, free of magnetic correlations, the conduction electrons scatter on -disordered magnetic moments and ρ_{mag} is expected to be roughly temperature independent. In a magnetically ordered state, ρ_{mag} decreases with temperature in a way characteristic for magnetic excitations in a particular material, especially magnons, and ρ_{mag} should vanish in the low temperature limit^{2,3}.

The magnetic periodicity of antiferromagnets usually does not coincide with the crystallographic (chemical) one. As a result of the spin-density wave exchange potential the Fermi surface is truncated by energy gaps. This leads to a reduction of effective charge-carriers number and consequent increase of resistivity at the Néel temperature, T_N ⁵. Such effect can be found both in itinerant antiferromagnets like Cr⁶ and in lanthanide localized-moment systems⁵. The resistivity can be than described as^{5,7}:

$$\rho = \frac{\rho_0 + \rho_{e-p} + \rho_{mag}}{1 - g \cdot m(T)} \quad (2),$$

where $m(T)$ is a normalized sublattice (staggered) magnetization and the truncation parameter g characterizes an effective reduction of the number of conduction electrons due to the Fermi surface gapping, which enhances the resistivity even in the low temperature limit.

When a sufficiently strong magnetic field is applied the antiferromagnet undergoes at the critical field H_c a metamagnetic transition (MT) to PM state where the periodicity of antiferromagnetic (AFM) structure is removed. Consequently, AFM gaps on Fermi surface are closed and the electrical conductivity correspondingly recovered. This mechanism is responsible for the field-induced change of resistivity in antiferromagnets due to MT.

Ising antiferromagnets⁸ and uniaxial uranium-based antiferromagnets, which exhibit Ising-like behavior⁹⁻¹², usually undergo at sufficiently low temperatures MT, which is a first-order magnetic phase transition (FOMPT) from AFM to PM state with field-forced ferromagnetic-like aligned magnetic moments, which is called a field polarized paramagnet

(PPM) regime^{13,14}. This transition is accompanied by a dramatic drop of resistivity^{15,16} between the AFM state and the PPM regime, in which ρ_{mag} practically vanishes similar to ρ_{mag} in ferromagnets in the low-temperature limit.

At higher temperatures the applied magnetic field induces fluctuations -in the AFM state. These fluctuations are gradually enhanced with increasing the magnetic field up to H_c and MT is a second-order magnetic phase transition (SOMPT). The conduction electrons scatter on the fluctuations which yields a progressively increasing contribution to ρ_{mag} ¹⁷ in fields up to H_c where a peak in the field dependence of resistivity has been found by calculations¹⁸ and experiment, e.g. on V_5S_8 ¹⁹. Exact theoretical determination of this contribution is however difficult. Detailed knowledge of the character and evolution of fluctuations from the AFM state with magnetic field determined by the hierarchy of exchange interactions in an actual material, is needed.

Owing to the weak exchange coupling of the conduction electrons with the localized $4f$ -electrons the corresponding magnetic contributions to resistivity in lanthanide compounds are small despite that the magnetic moments of lanthanide ions with $4f$ -electrons are large. Much larger ρ_{mag} values and consequent larger resistivity changes across MT can be expected in materials with strong coupling. This is likely in transition-metal or light-actinide compounds, which are characterized by the magnetic d - or $5f$ -electron states, respectively, at E_F , which implies a strong coupling with the conduction electrons.

The ordinary Hall effect turned out to be a useful tool for determination of charge-carrier density in nonmagnetic materials and played an important role in the early-years of semiconductor physics research and the related solid-state electronics. The recent rapid development of spintronics is focused mainly on the anomalous (also called extraordinary) Hall effect (AHE), which is a consequence of spin-orbit coupling in magnetic materials. The Hall resistivity of magnetic materials, $\rho_H(H)$ is described empirically as a sum of two terms; the normal and extraordinary Hall resistivity, respectively²⁰⁻²³:

$$\rho_H = R_H \cdot \mu_0 H = R_o \cdot \mu_0 H + R_e \cdot M \quad (3),$$

where R_o and R_e are the normal and the extraordinary Hall coefficient, respectively, H is the magnetic field and M is the volume magnetization. AHE is usually much larger than the ordinary Hall effect.

A large amount of papers presenting the results of measuring various transport properties of magnetic materials can be found in journals. Results of measurements of various properties obtained on different-quality samples of a particular compound, however, do not allow to employ complementarity of information, which could be deduced from reliable data on various measured properties on one, well defined, sample.

We made efforts to obtain a complete palette of data sets of the above mentioned electrical transport properties measured along the main crystallographic directions of a UIrSi_3 single crystal over a wide range of temperatures and magnetic fields. Here we discuss the new results together with the already published magnetization and specific-heat data¹⁰ in terms of a complex antiferromagnetism in a tetragonal non-centrosymmetric lattice. The Ising character of antiferromagnetism indicated by the anisotropy of magnetization and specific-heat data with respect to the direction of the magnetic field has been confirmed by constant zero longitudinal magnetoresistance in magnetic fields applied perpendicular to the

crystallographic c -axis, which is the easy magnetization direction. Consequently, we have focused on measurements of $\rho_{[100]}$, $\rho_{[001]}$ and ρ_H in fields applied along c -axis.

All three resistivities were found to be sensitive to magnetic-phase transitions in UIrSi₃. They exhibit considerable anomalies of $\rho(T)$ and $\rho_H(T)$ dependencies in various magnetic fields at corresponding critical temperatures $T_N(H)$ and $\rho(H)$ and $\rho_H(H)$ isotherm at corresponding critical fields of MT, H_c , respectively. The observed change of polarity of the $\Delta\rho(T)$, $\Delta\rho_H(T)$ and $\Delta\rho_H(H)$ steps at the temperature and magnetic field where the FOMPT changes to a SOMPT may offer a unique criterion for determination of the tricritical point (TCP) in the magnetic phase diagram of UIrSi₃.

The unique sensitivity of electrical transport to details in AFM arrangements of magnetic moments is employed in the well-known giant-magnetoresistance applications, especially in spintronics. It offers also an excellent probe of microscopic details of AFM ordering in bulk crystals. The same is true also in the UIrSi₃ case where an anomaly in the longitudinal magnetoresistance in the c -axis magnetic field reveals phenomena as, e.g. transition between two AFM states, which may be invisible for magnetization measurements similar to the CePtSn case²⁴⁻²⁶.

Experimental

UIrSi₃ single crystal has been prepared by the floating zone melting method in a commercial four-mirror optical furnace with halogen lamps each 1kW (modelFZ-T-4000-VPM-PC, Crystal Systems Corp., Japan). In the first step, a polycrystalline material of UIrSi₃ was synthesized by arc-melting from the stoichiometric amounts of pure elements U (3N, further treated by Solid State Electrotransport^{27,28}, Ir (4N), and Si (6N) in Ar (6N) protective atmosphere. Any sign of evaporation was not detected during the melting. Then, a precursor in the form of a 50 mm long rod was prepared by arc melting in a special water-cooled copper mould at identical protective conditions. Quartz chamber of the optical furnace was evacuated by a turbomolecular pump to 10⁻⁶ mbar before the crystal growth process. In order to desorb gases from the surface of the precursor, the power of the furnace was increased gradually up to 30% of maximum power (far below from the melting at ~54% of power) and precursor was several times passed through the hot zone while continuously evacuating. After the degas process and evacuation, the quartz chamber was quickly filled with high purity Ar (6N). The whole growth process was performed with Ar flow of 0.25 l/min and pressure of ~2 bar. A narrow neck was created in the beginning of the growth process by variation of the speed of the upper and bottom pulling shafts. The pulling rate was very slow, only 0.5 mm/h, and without rotation. A large single crystal of the cylindrical shape with length ~50 mm and diameter 4 mm was obtained. High quality and orientation of the single crystal was verified by Laue method (Fig. 1). The chemical composition of single crystal was verified by a scanning electron microscopy (SEM) using a Tescan Mira I LMH system equipped with an energy-dispersive X-ray detector (EDX) Bruker AXS. The analysis revealed a single phase single crystal of 1:1:3 composition. Detailed surface analysis did not detect any foreign phases.

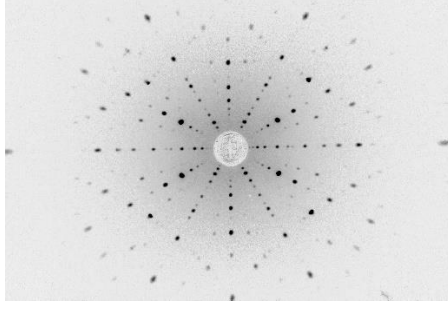


FIG. 1. Laueogram of the UIrSi₃ single crystal oriented along [110].

The resistivity, Hall resistivity, magnetization and specific heat measurements were carried out with a physical property measurement system (PPMS, Quantum Design Inc.) in magnetic fields applied along the c -axis up to 9 T. For determination of T_N from the temperature dependence of specific heat the point of the balance of entropy released at the phase transition method was used. Specific heat was measured in basal plane (sample mass ~ 11 mg) with applied magnetic field along c -axis. Measurements with application of magnetic field along c - and a -axis were carried out for measurement of magnetization (sample mass ~ 11 mg). Resistivity measurements were performed with electrical current along c - and a -axis in two bar-shape samples ($0.75 \times 0.73 \times 1.8$ mm³ for current along a -axis and $0.78 \times 0.55 \times 1.1$ mm³ along c -axis) with magnetic field along c -axis. Hall resistivity was measured with a plate-shaped sample (with diameters: 1.2 mm) for magnetic field up to ± 14 T with assembly: current along a -axis, magnetic field along c -axis.

Results and Discussion

The observed anisotropy of the temperature dependence of the electrical resistivity, $\rho(T)$ (see Fig. 2) indicates an anisotropic Fermi surface of UIrSi₃. The resistivities $\rho_{[100]}(T)$ and $\rho_{[001]}(T)$ for current $i \parallel [100]$ and $[001]$, respectively, increase with increasing temperature above T_N and gradually saturate (the curvature and tendency to saturation is more pronounced in the $\rho_{[001]}(T)$ dependence). This resembles behavior of transition metals and their compounds characterized by a narrow d -electron band crossing the Fermi level (E_F), which was explained by an s - d scattering mechanism as proposed by Mott²⁹ and Jones³⁰. We tentatively suppose that the resistivity of U intermetallics characterized by a narrow 5f-electron band crossing the E_F could be considered within an analogous s - f scattering model.

The negative curvature of both, $\rho_{[100]}(T)$ and $\rho_{[001]}(T)$ observed at high temperatures suddenly changes to a convex dependence at the same characteristic temperature, which coincides with the T_N value determined from specific-heat data (see inset of Fig. 2). The RRR values are 34 and 14, respectively.

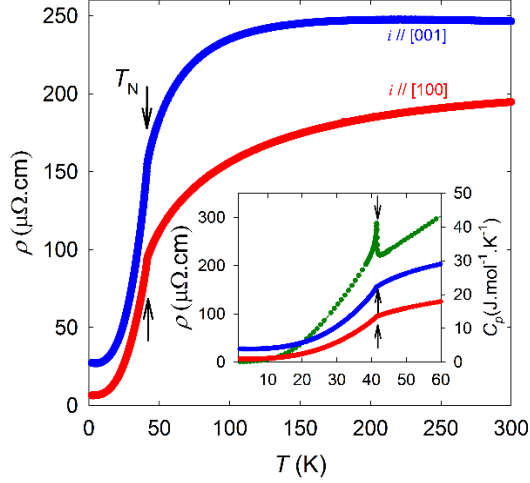


FIG. 2. Temperature dependence of the electrical resistivity of UIrSi_3 for electrical current parallel to the $[100]$ and $[001]$ direction, respectively. Inset: a low-temperature detail including also the corresponding specific-heat C_p vs. T (green points) plot. The arrows mark T_N .

When we apply the magnetic field along the $[001]$ direction the T_N -related anomaly in the $\rho_{[100]}(T)$ and $\rho_{[001]}(T)$ dependences are shifted to lower temperatures with increasing field so that they follow the corresponding specific-heat anomaly (see Fig. 3). The resistivity anomaly simultaneously develops with increasing the field from just a negative $\partial\rho/\partial T$ change in zero field to a clear positive $\Delta\rho$ step in 5 T. T_N is associated with the maximum of $\partial\rho/\partial T$. In 6 T we suddenly observe a negative $\Delta\rho$ step at T_N , which is exhibited also by the zero-field-cooled (ZFC) curves measured in 7 T. The 8-T $\rho_{[100]}(T)$ and $\rho_{[001]}(T)$ curves are smooth showing no sharp anomaly within the entire temperature range. A detailed view of the evolution $\rho_{[001]}(T)$ curves in fields from 5 to 8 T is displayed in Fig. 4 together with the corresponding magnetization $M(T)$ dependences which exhibit a positive ΔM step at T_N in the fields of 5 and 6 T, respectively which is followed by a decay of the paramagnet magnetization with further increasing temperature. The T_N -related anomalies in the $\rho_{[001]}(T)$ and $M(T)$ curves measured in 6 T exhibit a temperature hysteresis, which is characteristic of a first-order phase transition. In contrary, the T_N -related anomalies in fields up to 5 T show no hysteresis.

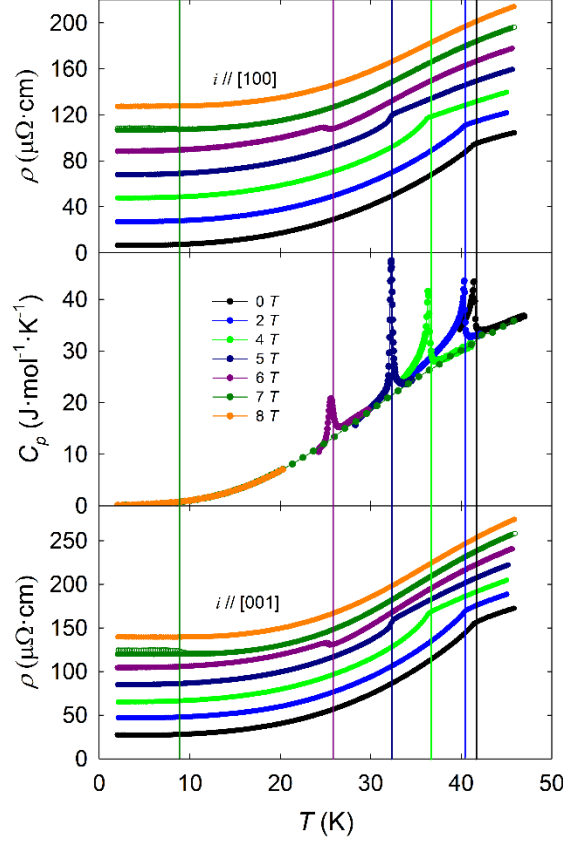


FIG. 3. Temperature dependence of the electrical resistivity for current parallel to the [100] and [001] direction (top and bottom panel, respectively) and specific heat (middle panel) of UIrSi_3 below 60 K in the magnetic field applied in the [001] direction. The ρ vs. T curves measured in different fields are mutually shifted by $20 \mu\Omega\cdot\text{cm}$ along the vertical axis for clarity. The actual vertical scale corresponds to the 0-T curve. The colored vertical lines represent the T_N values corresponding to the actual applied magnetic fields. The 7-T line corresponds to the bifurcation point of the FC and ZFC resistivity curves.

The Hall resistivity, ρ_H , in field parallel to [001] is also sensitive to the PM \leftrightarrow AFM transition at T_N as can be seen in Fig. 5. The T_N -related anomaly in the $\rho_H(T)$ corresponding to a gradually increasing magnetic field undergoes a development analogous to the normal-resistivity case. It is gradually shifted to lower temperatures in coincidence the T_N -related specific-heat and magnetization anomalies. The Hall resistivity anomaly simultaneously develops with increasing the field from a positive $\partial\rho_H/\partial T$ change in 1 T to a clear negative $\Delta\rho_H$ step in 5 T. T_N coincides with the minimum of $\partial\rho_H/\partial T$ and roughly with the maximum of $\partial M/\partial T$. Also the Hall resistivity exhibits contrast between the T_N -related anomalies in fields up to 5 T and those measured in higher fields. In 6 T we suddenly observe a positive $\Delta\rho_H$ step at T_N with temperature hysteresis. The observed qualitative changes of the T_N -related anomalies in the corresponding $M(T)$, $\rho_{[100]}(T)$, $\rho_{[001]}(T)$ and $\rho_H(T)$ dependences in fields between 5 and 6 T may be considered in connection with the conclusion in Ref. 10 that the change from SOMPT to FOMPT happens at TCP which has been estimated at $\mu_0 H_{tc} \sim 5.8$ T, $T_{tc} \sim 28$ K.

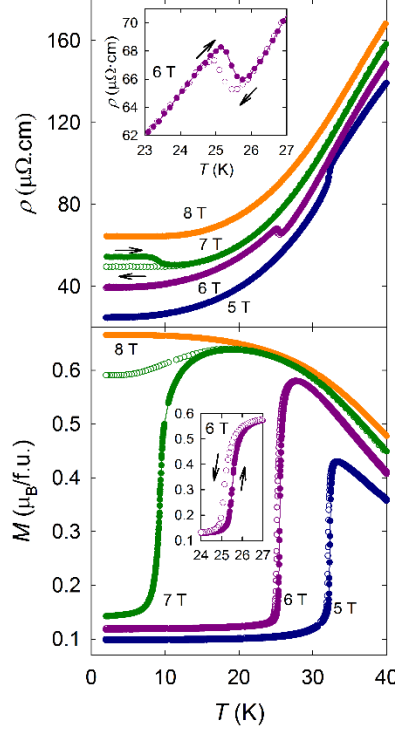


FIG. 4. Temperature dependences of the electrical resistivity $\rho_{[001]}$ (upper panel) and magnetization M (lower panel) of UIrSi_3 measured in the magnetic field of 5, 6, 7 and 8 T, respectively, applied in the [001] direction. For 7 T the ZFC (full symbols) and FC (open symbols) $M(T)$ and $\rho(T)$ curves, respectively, bifurcate below T_N . The $\rho(T)$ curves measured in different fields are mutually shifted by $15 \mu\Omega\cdot\text{cm}$ along the vertical axis for clarity. The displayed vertical scale corresponds to the 5-T curve. Inset of lower panel: detail of the hysteresis of the transition in 6 T. The arrows represent the type of field sweep.

The ZFC $\rho_H(T)$ curve measured in 7 T shows also a step, which is however considerably larger. Similar to normal resistivity and magnetization behavior, the 8-T $\rho_H(T)$ curve is smooth showing no sharp anomaly within the entire temperature range. The 8-T field is sufficiently higher than $\mu_0 H_c$ (7.3 T) at 2 K¹⁰ to destroy entirely the AFM ordering in the ZFC sample and recover the PM state (the PPM regime at temperatures $T < T_{tc}$ while cooling the sample in 8 T prevents any transition to the AFM ordering, i.e. the sample remains PM. That is why the corresponding 8-T field-cooled (FC) and ZFC $M(T)$, $\rho_{[100]}(T)$, $\rho_{[001]}(T)$, $\rho_H(T)$ curves, respectively, are identical and exhibit no T_N -related anomaly (see Figs. 3 and 4).

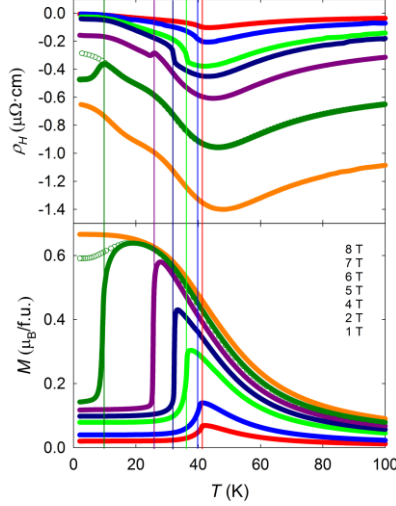


Fig. 5. Temperature dependence of Hall resistivity ρ_H vs. T (upper panel) and magnetization M vs. T (lower panel) of UIrSi_3 in several magnetic fields applied in the [001] direction. The ρ_H vs. T and M vs. T plots in corresponding magnetic fields are in the same colors. The colored vertical lines represent the T_N values determined by specific-heat measurements. The 7-T vertical line corresponds to the bifurcation point of the ZFC (full symbols) and FC (open symbols) ρ_H vs. T and M vs. T curves, respectively. The 6-T, 7-T and 8-T plots in upper panel are vertically shifted by - 0.1, - 0.4, - 0.8 $\mu\Omega\cdot\text{cm}$, respectively.

The corresponding ZFC and FC $M(T)$, $\rho_{[100]}(T)$, $\rho_{[001]}(T)$, $\rho_H(T)$ curves measured in 7 T bifurcate in the vicinity of T_N . This is reflecting the large field hysteresis of the MT reported in Ref. 10 which extends around 7 T at low temperatures. When cooling UIrSi_3 in 7 T the $M(T)$ values reach the maximum value at $\sim 20\text{K}$ then they decrease by about 10% which indicates that the low-temperature FC state is a somewhat disturbed PPM which, however, exhibits considerably lower resistivity than the low-temperature ZFC state (probably the AFM ground state) which is associated with a higher resistivity due to the Fermi surface truncated by energy gaps caused by different periodicity of the crystallographic and AFM lattice.

The entire $\rho_H(T)$ dependences measured between 2 and 100 K in fields up to 8 T show a broad valley. The temperature of its minimum roughly coincides with the temperature of the $\partial M/\partial T$ minimum. The ρ_H values are negative, as expected for the ordinary Hall effect in case of electron conductivity in metals. The positive values in the 8-T and FC 7-T $\rho_H(T)$ dependences at low temperatures reflect large positive contributions due to AHE in UIrSi_3 in the PPM state.

In Fig. 6, $\rho_{[100]}(H)$, $\rho_{[001]}(H)$ data at representative temperatures are displayed over the range of c -axis magnetic fields including MTs in UIrSi_3 . In the lower panels results obtained at $T < T_{lc}$ at which FOMPT takes place are displayed. The $\rho_{[001]}(H)$ curves in the vicinity of H_c qualitatively resemble the corresponding magnetization curves in Ref. 10 taken with negative sign, i.e. the resistivity sharply drops at H_c when sweeping the magnetic field up and exhibits the asymmetric hysteresis of MT when sweeping the field down. If the bump below 4 T seen at lowest temperatures, which will be discussed later, is ignored at the moment, $\rho_{[001]}(H)$ in fields below the hysteretic MT is practically constant. The MT-related anomalies on the corresponding $\rho_{[100]}(H)$ curves representing transverse magnetoresistance are

qualitatively very similar. The slight upturn in fields below MT reflects the quadratic contribution ($\sim H^2$) due to the effect of magnetic field on electrons moving in the plane perpendicular to the field direction.

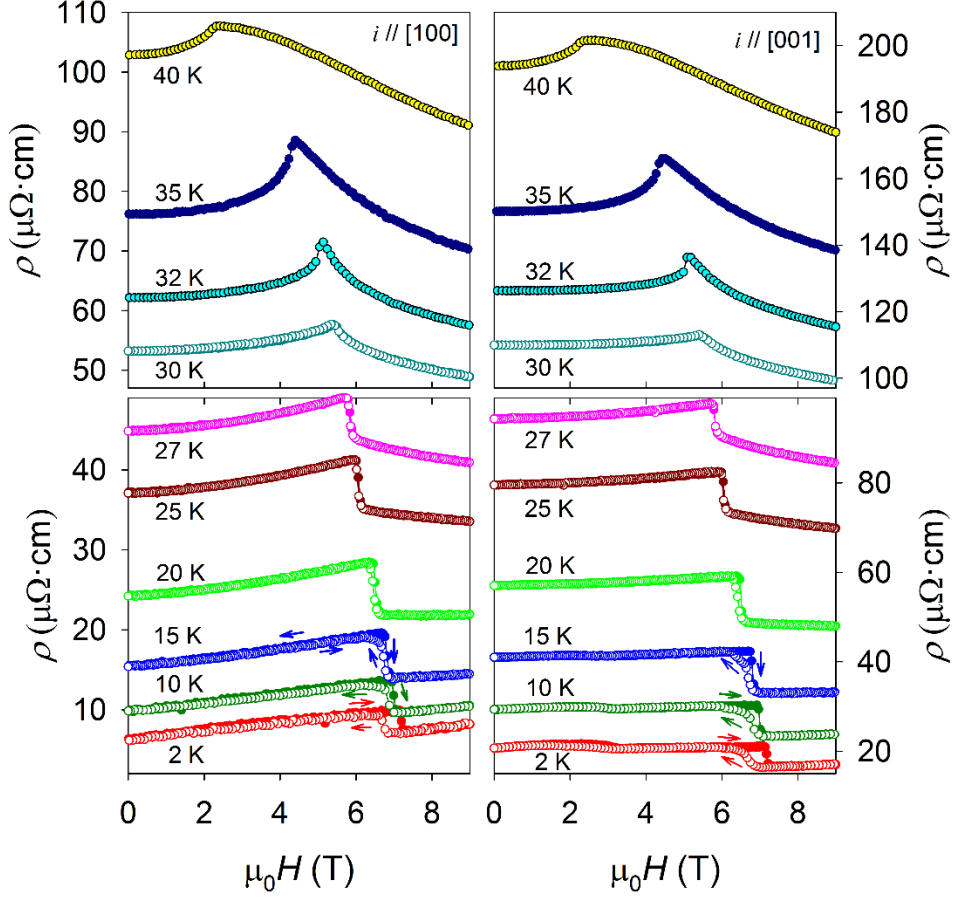


FIG. 6. The electrical resistivity of UIrSi₃ at selected temperatures for current parallel to the [100] (left panel) and [001] (right panel) direction as function of the magnetic field applied in the [001] direction. The $\rho(H)$ curves measured at different temperatures (10 K – 40 K) and for current parallel to [100] ([001]) are mutually shifted by 2 $\mu\Omega\cdot\text{cm}$ (6 $\mu\Omega\cdot\text{cm}$) along the vertical axis for clarity. Where needed the arrows show the direction of field sweep.

The $\rho_{[100]}(H)$, $\rho_{[001]}(H)$ curves in the upper panels of Fig. 6 were measured at temperatures between T_{tc} and T_{N} . At these temperatures UIrSi₃ undergoes a field-induced SOMPT (AFM \leftrightarrow PM). A dramatic difference in the electrical resistivity response in comparison to the lower-temperatures FOMPT's is clearly seen. Here the resistivity considerably increases with increasing field up to the maximum value $\rho(H_c)$. In fields beyond H_c the resistivity values decay fast with increasing H yielding a negative magnetoresistance well above H_c . Contrary to FOMPT's these transitions have no hysteresis.

The Hall-resistivity isotherms $\rho_{\text{H}}(H)$ measured at temperatures below 28 K show a sudden positive $\Delta\rho_{\text{H}}(H)$ step at H_c and asymmetric hysteresis, being at lowest temperatures very similar to the magnetization behavior around the FOMPT at H_c ¹⁰. In contrary, the $\rho_{\text{H}}(H)$ curves measured at temperatures higher than 28 K exhibit a slightly rounded negative step at H_c and no field hysteresis. The step gradually smears out with increasing temperature to

disappear at temperatures around 40 K. Note that $\Delta\rho_H(H)$ decreases (but does not scale) with the decreasing corresponding $\Delta M(H)$ step.

The observed opposite polarity of the Hall effect step accompanying FOMPT and SOMPT, respectively, allows precise determination of the TCP, which separates the FOMPT and SOMPT sections of the magnetic phase diagram, as a point where the polarity changes.

As mentioned above also the anomalies in $\rho_{[100]}(T)$, $\rho_{[001]}(T)$ and $\rho_H(T)$ temperature dependences, respectively, measured in fields 5 and 6 T exhibit at T_N step-like anomalies of opposite polarity (see in Figs. 4, 5 and 7). Since the TCP is located at $\mu_0 H_{tc} \sim 5.8$ T, $T_{tc} \sim 28$ K the opposite-polarity anomalies measured in fields 5 and 6 T are on opposite sides of the TCP, namely 5 T in the SOMPT section and 6 T in the FOMPT section of the magnetic phase diagram. One may expect that measurements in fine-tuned fields around 5.8 T would enable precise determination of TCP also from these data.

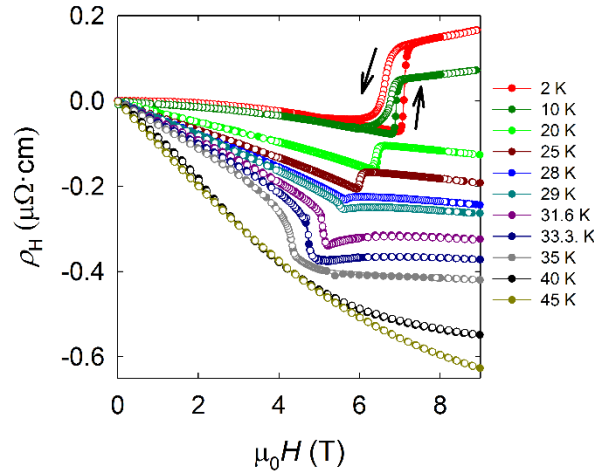


FIG. 7. The Hall resistivity of UIrSi_3 at selected temperatures as a function of the magnetic field applied in the $[001]$ direction. Where needed the arrows show the direction of field sweep.

The key question of our present study is about the origin of the appearance of a SOMPT and a FOMPT in an anisotropic uniaxial antiferromagnet which has features of an Ising system. Closer inspection of $M(T)$, $\rho_{[001]}(T)$ and $\rho_H(T)$ measured in different magnetic fields allows us to see what is going on with the system of magnetic moments when cooling or heating. When cooling down in a field of 8 T we record at 2 K the highest M and ρ_H values, the lowest ρ ones and the magnetization is almost saturated. Also, the magnetization curve measured at 2 K is saturated above M_T , which is below 8 T. The system at 2 K and 8 T in both cases is in a paramagnetic state with magnetic moments (highly) polarized by the magnetic field, i.e. PPM regime. The 7-T $\rho_{[001]}(T)$ and $\rho_H(T)$ data at $20 < T < 28$ K are almost identical with the 8-T behavior, i.e. the moments become polarized similarly. The polarization is assisted by strong uniaxial anisotropy of UIrSi_3 . Our preliminary neutron diffraction experiment is zero magnetic field indicates that the U magnetic moments in the AFM state are oriented along the c -axis which is consistent with the strong uniaxial anisotropy.

For explanation of the above presented findings we propose the following scenario:

FOMPTs in UIrSi₃ are the AFM \leftrightarrow PPM transitions whereas the SOMPTs are the AFM \leftrightarrow PM, where PM stands for a normal paramagnetic state with normal thermal fluctuations of magnetic moments. The PPM regime at low temperatures, which is characterized by magnetic moments aligned along the field direction, resembles (and is frequently wrongly quoted) as a ferromagnetic state. In the case of full polarization, it yields zero contribution to electrical resistivity with, on the other hand, a large contribution to anomalous Hall resistivity. The TCP separates the FOMPT and SOMPT regions in the magnetic phase diagram. The relation between the characteristic values of electrical resistance and anomalous Hall resistance of the three states (regimes) are:

$$\rho^{PM} > \rho^{AFM} > \rho^{PPM} \quad (4),$$

$$\rho_H^{PM} < \rho_H^{AFM} < \rho_H^{PPM} \quad (5),$$

respectively.

To confirm universality is the scenario, which is characterized by the change of polarity of $\Delta\rho(T)$, $\Delta\rho_H(T)$ and $\Delta\rho_H(H)$ at TCP, requires analogous investigation of electrical transport in some representative Ising-like antiferromagnets in the suspected magnetic-phase space.

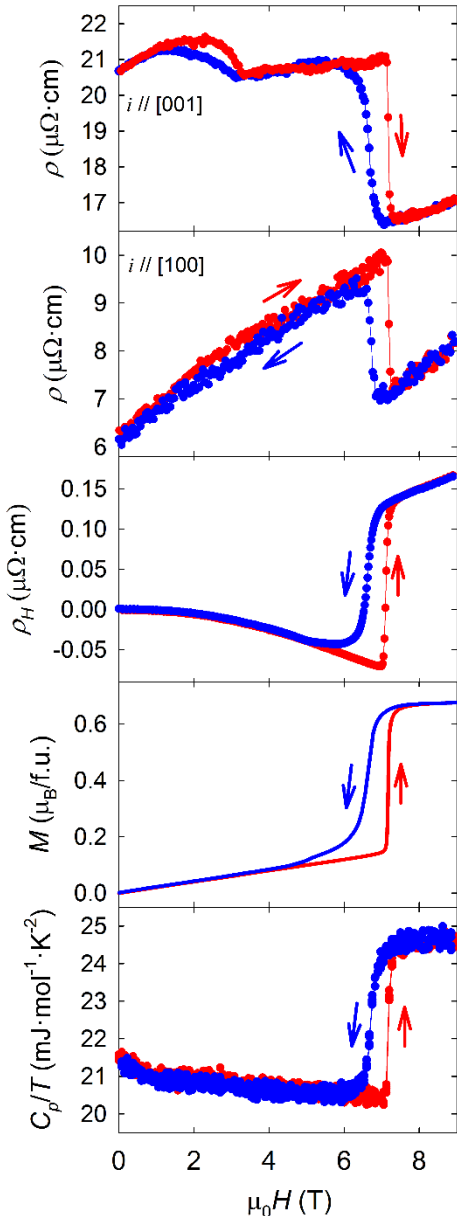


FIG. 8. From top to bottom panel:

- electrical resistivity for $J//[001]$
- electrical resistivity for $J//[100]$
- hall resistivity
- magnetization
- specific heat divided by temperature

of UIrSi₃ at 2 K as functions of the magnetic field applied in the [001] direction.

There is another important result worth to mention, which is connected specifically with the behavior of UIrSi₃, which becomes evident when inspecting Fig. 8. In particular, one can see a pronounced anomaly in the $\rho_{[001]}$ vs. H plot in fields between 0 and 4 T,

which is somewhat reflected also in the $\rho_{[100]}$ behavior. On the other hand, no indication is observed in field dependences of magnetization, Hall resistance and specific heat measured on an identical sample. At the moment we have no clue for an explanation of this c -axis field-induced effect which has been indicated only by measuring electrical resistivity, which in some specific cases could reveal phenomena as, e.g. a transition between two AFM states (being invisible for magnetization measurements similar to the CePtSn case²⁵⁻²⁷). The

sensitivity of electrical resistivity in U compounds including UIrSi₃ is enhanced due to the strong exchange coupling of the conduction electrons and the U 5*f*-electrons having states at the Fermi surface. Detailed microscopic studies, mainly using the neutron scattering are desired to shed some light on the unknown, probably AFM phase, related to the resistivity anomalies in *c*-axis fields up to 4 T.

In Fig. 9, the revised magnetic phase diagram of UIrSi₃ in the magnetic field applied along the *c*-axis is depicted, including results from Ref. 10 and from this paper. The additional unknown “AFM1” phase indicated in fields between 0 and 4 T by $\Delta\rho_{[001]}$ measurements is included.

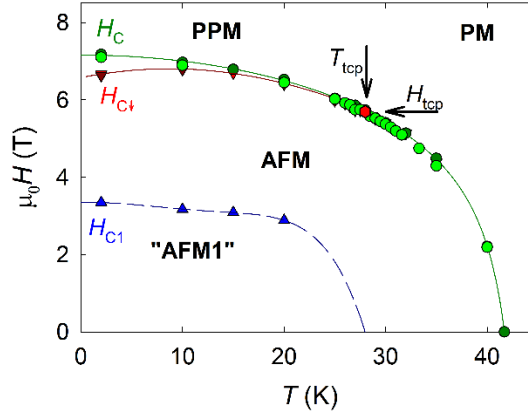


FIG. 9. Revised magnetic phase diagram of UIrSi₃ in the magnetic field applied along the *c*-axis.

Conclusions

We have performed a detailed study of the electrical resistance and Hall resistance of the Ising non-centrosymmetric antiferromagnet UIrSi₃ as functions of temperature and magnetic field. The obtained results demonstrate that the electrical transport properties serve as a sensitive probe of magnetic phase transformations in antiferromagnets sometimes hardly detectable by other methods.

We have observed that the unequivocally different character of FOMPT and SOMPT is reflected in the dramatically different transport properties in the neighborhood of corresponding critical temperatures T_N and magnetic fields H_c . Considering the magnetic parts of electrical resistivity and Hall resistivity, we have suggested a scenario which may successfully explain the observed change of polarity of the $\Delta\rho(T)$, $\Delta\rho_H(T)$ and $\Delta\rho_H(H)$ steps between FOMPT and SOMPT and allow precise determination of the TCP in the magnetic phase diagram of Ising antiferromagnets exhibiting tricriticality. These findings stimulate further analogous experiments on Ising-like antiferromagnets dedicated to test the universality of the scenario. Magneto-optic experiments would be useful for deeper understanding of the underlying mechanism of AHE in UIrSi₃.

Neutron-scattering studies are planned to reveal the microscopic aspects of magnetism in this intriguing material.

Acknowledgments

This research is supported by Grant Agency of Charles University (GAUK) by project no. 188115, the Czech Science Foundation, grant No. P204/15-03777S and the Japan Society for the Promotion of Science (JSPS) KAKENHI with the grant nos. 15K05156 and 15KK0149. Experiments were performed in the Materials Growth and Measurement Laboratory MGML (<http://mgml.eu>). The authors are indebted to Dr. Ross Colman for critical reading and correcting the manuscript.

References

- ¹ A. J. Dekker, *J. Appl. Phys.* **36**, 906 (1965).
- ² T. Kasuya, *Prog. Rep. Phys. (Kyoto)* **16**, 227 (1959).
- ³ D. L. Mills and P. Lederer, *Phys. Chem. Solids* **27**, 1805 (1966).
- ⁴ E. Jobiliong, J. S. Brooks, E. S. Choi, H. Lee, and Z. Fisk, *Phys. Rev. B* **72**, (2005) 104428.
- ⁵ R. J. Elliott and F. A. Wedgwood, *Proc. Phys. Soc.* **81**, 846 (1963).
- ⁶ S. Arajs, R. V. Colvin, and M. J. Marcinkowski, *J. Less-Common Metals* **4**, 46 (1962).
- ⁷ V. Sechovský, L. Havela, K. Prokeš, H. Nakotte, F. R. de Boer, and E. Brück, *J. Appl. Phys.* **76**, 6913 (1994).
- ⁸ D. P. Landau, *Phys. Rev. Lett.* **28**, 449 (1972)
- ⁹ E. Brück, H. P. Vandermeulen, A. A. Menovsky, F. R. De Boer, P. F. De Châtel, J. J. M. Franse, J. Perenboom, T. Berendschot, H. Van Kempen, L. Havela, and V. Sechovský, *J. Magn. Magn. Mater.* **104**, 17 (1992).
- ¹⁰ J. Valenta, F. Honda, M. Vališka, P. Opletal, J. Kaštil, M. Mišek, M. Diviš, L. Sandratskii, J. Prchal, and V. Sechovský, *Phys. Rev. B* **97**, 144423 (2018).
- ¹¹ K. Shrestha, D. Antonio, M. Jaime, N. Harrison, D. S. Mast, D. Safarik, T. Durakiewicz, J. C. Griveau, and K. Gofryk, *Sci. Rep.* **7**, 6642 (2017).
- ¹² R. L. Stillwell, I. L. Liu, N. Harrison, M. Jaime, J. R. Jeffries, and N. P. Butch, *Phys. Rev. B* **95**, 014414 (2017).
- ¹³ W. Knafo, R. Settai, D. Braithwaite, S. Kurahashi, D. Aoki, and J. Flouquet, *Phys. Rev. B* **95**, 014411 (2017).
- ¹⁴ J. Pospisil, Y. Haga, Y. Kohama, A. Miyake, S. Kambe, N. Tateiwa, M. Valiska, P. Proschek, J. Prokleska, V. Sechovský, M. Tokunaga, K. Kindo, A. Matsuo, and E. Yamamoto, *Phys. Rev. B* **98**, 014430 (2018).
- ¹⁵ E. Brück, H. Nakotte, F. R. de Boer, P. F. de Châtel, H. P. van der Meulen, J. J. M. Franse, A. A. Menovsky, N. H. Kim-Ngan, L. Havela, V. Sechovsky, J. A. A. J. Perenboom, N. C. Tuan, and J. Sebek, *Phys. Rev. B* **49**, (1994) 8852.
- ¹⁶ H. Nakotte, E. Brück, F.R. de Boer and A.J. Riemersma L. Havela and V. Sechovsky, *Physica B* **179**, (1992) 269-271.
- ¹⁷ H. Yamada and S. Takada, *Prog. Theor. Phys.* **49**, (1973) 1401.
- ¹⁸ K. Usami, *J. Phys. Soc. Jpn.* **45**, (1978) 466.
- ¹⁹ H. Nozaki, Y. Ishizawa, *Physics Letters* **63A**, (1977) 131.
- ²⁰ E.M. Pugh, *Phys. Rev.* **36**, (1930) 1503.
- ²¹ N. Nagaosa, J. Sinova, S. Onoda, A. H. MacDonald, and N. P. Ong, *Rev. Mod. Phys.* **82**, (2010) 1539.

- ²² C.M. Hurd, The Hall Effect in Metals and Alloys, *Plenum Press*, New York, 1972.
- ²³ L. Berger, G. Bergmann, in: C.L. Chien, C.R. Westgate (Eds.), The Hall Effect and its Applications, *Plenum Press*, New York, 1980, p. 55 and references therein.
- ²⁴ D.R. Noakes, G.M. Kalvius, *Physica B* **289–290**, (2000) 248.
- ²⁵ B. Janoušová, V. Sechovský, K. Prokeš, T. Komatsubara, *Physica B* **328**, (2003) 145.
- ²⁶ J. Prokleška, B. Detlefs, V. Sechovský, M. Míšek, *J. Magn. Magn. Mater.* **322**, (2010) 1120.
- ²⁷ Y. Haga, T. Honma, T. Yamamoto, H. Ohkuni, Y. Onuki, M. Ito, and N. Kimura, *Japanese Journal of Applied Physics* **37**, 3604 (1998).
- ²⁸ J. Pospíšil, K. Prokeš, M. Reehuis, M. Tovar, J. P. Vejpravová, J. Prokleška, and V. Sechovský, *Journal of the Physical Society of Japan* **80**, 084709 (2011).
- ²⁹ N.F. Mott, *Proc. R. Soc.* **A153**, (1936) 699.
- ³⁰ H. Jones, *Hdb. Physik* Vol. 2 XIX (Berlin: Springer Verlag 1956), p. 266.